

# Transport of Aromatic Molecules in NaY Zeolite Powders

Xenon-129 NMR is used to probe macroscopic distributions of aromatic molecules adsorbed in a packed bed of 1- $\mu\text{m}$  NaY zeolite particles. Relative rates of guest transport through the intracrystalline (micro) and intercrystalline (macro) pores play a unique role in the axial distribution of sorbate molecules, such as hexamethylbenzene, in a zeolite powder. Xenon-129 NMR spectra show that a sharp HMB adsorption front advances through a bed of dehydrated NaY crystallites at 523 K. However, at 573 K or in the presence of coadsorbed water, HMB species disperse through the bed without forming a sharp boundary between adsorption zones.

When guest transport is controlled by pseudosteady-state diffusion in the macropores, axial penetration of the bed by vapor-phase guest species occurs in a sharp adsorption front. A shrinking-core transport model then quantitatively estimates the intracrystalline diffusivities of HMB in dehydrated and partially hydrated NaY zeolite of  $10^{-11}$  and  $10^{-13}$   $\text{m}^2/\text{s}$ , respectively, at 523 K. Xenon-129 NMR proves to be a powerful tool for probing adsorbed guest distribution in zeolites, allowing relative time scales to be established for transport of molecular guests in NaY powders.

**B. F. Chmelka**  
**J. V. Gillis**  
**E. E. Petersen**  
**C. J. Radke**

Department of Chemical Engineering  
University of California  
Berkeley, CA 94720

## Introduction

Transport and adsorption properties of reactant species in small pores are important to the performance of heterogeneous catalysts. The mobility of molecular guests establishes reactant accessibility to active sites within the porous matrix and, in so doing, affects species distribution within the catalyst particles. Distributions of adsorbed guest molecules in zeolite cavities are known, for instance, to depend on catalyst treatment conditions (Kondis and Dranoff, 1971; Cohen de Lara, 1980; Kärger et al., 1981; Gedeon et al., 1988), which affect the internal mass transfer properties of molecular sieves. Recently, we measured the distributions of organic adsorbates, namely benzene, 1,3,5-trimethylbenzene (TMB), and hexamethylbenzene (HMB) in NaY zeolite powder using  $^{129}\text{Xe}$  and multiple-quantum nuclear magnetic resonance spectroscopy (NMR) (Ryoo et al., 1987; de Menorval et al., 1990; Chmelka et al., in press). In this paper, we model quantitatively the distribution of hexamethylbenzene in NaY zeolite to establish the transport mechanisms re-

sponsible for the macroscopic adsorbate concentration profiles observed.

## Adsorbate Distributions by $^{129}\text{Xe}$ NMR

As a sensitive, nonreactive probe of supercage cavities within the crystalline zeolite matrix, room-temperature  $^{129}\text{Xe}$  NMR spectroscopy provides unique information on interparticle adsorbate heterogeneities in NaY powders. By monitoring the chemical shift of physisorbed  $^{129}\text{Xe}$ , distinct regions containing different concentrations of adsorbed guests can be identified within NaY zeolite samples.

All zeolite samples were prepared in 10-mm NMR tubes connected to a vacuum apparatus through a Kontes high-vacuum stopcock. NaY zeolite was synthesized according to the procedure of Breck (1982), with crystallinity confirmed by X-ray diffraction studies. Separate scanning electron microscopy experiments establish NaY crystallite grain diameters of 1–2  $\mu\text{m}$  (Chmelka, 1990). Before adding the adsorbate species, the NaY samples were dehydrated in the sample tubes by heating at 723 K under vacuum (ca.  $10^{-5}$  torr or  $1.3 \times 10^{-3}$  Pa)

Correspondence concerning this paper should be addressed to C. J. Radke.

overnight. For the rehydration study, coadsorbed water was introduced to dehydrated NaY by exposure to a low-moisture nitrogen atmosphere in a glove box for  $\approx 15$  min. After dehydration or partial rehydration, a known amount of organic adsorbate was introduced to the zeolite powder at room temperature to achieve the bulk loading desired. Adsorbate loadings were calculated from mass balances utilizing NaY supercage density and the masses of zeolite and organic guest materials. Solid HMB was stored at 273 K in a sidearm of the sample tube during dehydration and subsequently introduced mechanically under vacuum to the top of the zeolite sample volume. Without delay, the samples were placed in a furnace equipped with a programmable temperature controller, heated for a known period of time, and cooled to room temperature over a period of many hours. Xenon gas was then introduced into each sample at room temperature and allowed to equilibrate to a pressure of  $\approx 300$  torr (40 kPa). Room-temperature  $^{129}\text{Xe}$  NMR spectra were obtained on a spectrometer operating at 110.0 MHz. Each acquisition typically consisted of 2,000–4,000 free induction decay scans with a delay of 0.2 s between  $90^\circ$  pulses. The experiments employed a sweep width of 41.67 kHz with a digitizing time of 12  $\mu\text{s}$ . All  $^{129}\text{Xe}$  chemical shift values are referenced to the  $^{129}\text{Xe}$  signal of xenon gas at very low pressure (Fraissard et al., 1982) and are believed accurate to 0.5 ppm.

The  $^{129}\text{Xe}$  NMR spectrum shown in Figure 1a indicates a sharp, axial HMB adsorption front in a packed bed of micron-sized NaY crystallites. In this experiment, a limited amount of liquid HMB (0.5 HMB molecules per supercage) was brought into contact with the zeolite powder and held at 523 K for 2 h. The two well-resolved peaks at 109 ppm and 78 ppm in Figure 1a correspond to  $^{129}\text{Xe}$  physisorbed at ambient temperatures in adsorption zones with and without HMB guest species, as illustrated in the appended schematic diagrams of the NMR sample cell. Xenon exchange is slow between macroscopic zones containing different HMB loadings within the NaY zeolite supercages. From the frequency difference separating the two peaks, the time scale of the xenon exchange process is on the

order of  $10^{-4}$  s. This observation, coupled with  $^{129}\text{Xe}$  NMR experiments performed after thorough physical mixing of the packed bed, establishes that the  $^{129}\text{Xe}$  probe species averages the adsorbate loading within several NaY crystallites (each 1  $\mu\text{m}$  in diameter) at room temperature (Chmelka, 1990; Chmelka et al., in press). The well-resolved peaks, therefore, indicate essentially a step change in HMB concentration near the midpoint of the sample volume's longitudinal axis, with the nearly equal peak areas reflecting nearly equal numbers of xenon adsorption sites in the two regions. This is consistent with an average bulk loading of 0.5 HMB/cavity distributed so that the upper 50% of the bed contains one HMB molecule in nearly every supercage, while the lower 50% is devoid of adsorbed guests.

In contrast, no sharp adsorption front exists for HMB adsorbed at higher temperatures or for HMB in a bed of partially hydrated NaY zeolite. Thus, after reheating the dehydrated HMB/NaY sample of Figure 1a to 573 K for 4 h, the two discrete peaks coalesce to a single line at 94 ppm in Figure 1b. This is consistent with dispersal of HMB throughout the sample volume and indicates a macroscopically uniform guest distribution (Chmelka et al., in press).

The presence of coadsorbed water provides a dispersive influence on the distribution of aromatic guest species as well. In Figure 2, the  $^{129}\text{Xe}$  peak corresponding to the HMB adsorption zone in partially rehydrated NaY is shifted to 90 ppm, substantially upfield from its 109 ppm location in the dehydrated sample. In this case, the coadsorbed water produces a more shielded adsorption environment for the  $^{129}\text{Xe}$  probe atoms in NaY supercages containing HMB guest species. The nonzero  $^{129}\text{Xe}$  signal intensity between peaks at 78 and 90 ppm reflects a macroscopic distribution of NaY particles containing a range of different HMB loadings (0–1 HMB/supercage) near the boundary between distinct adsorption zones. Our objective is to elucidate the transport mechanism(s) responsible for the adsorbate distributions observed.

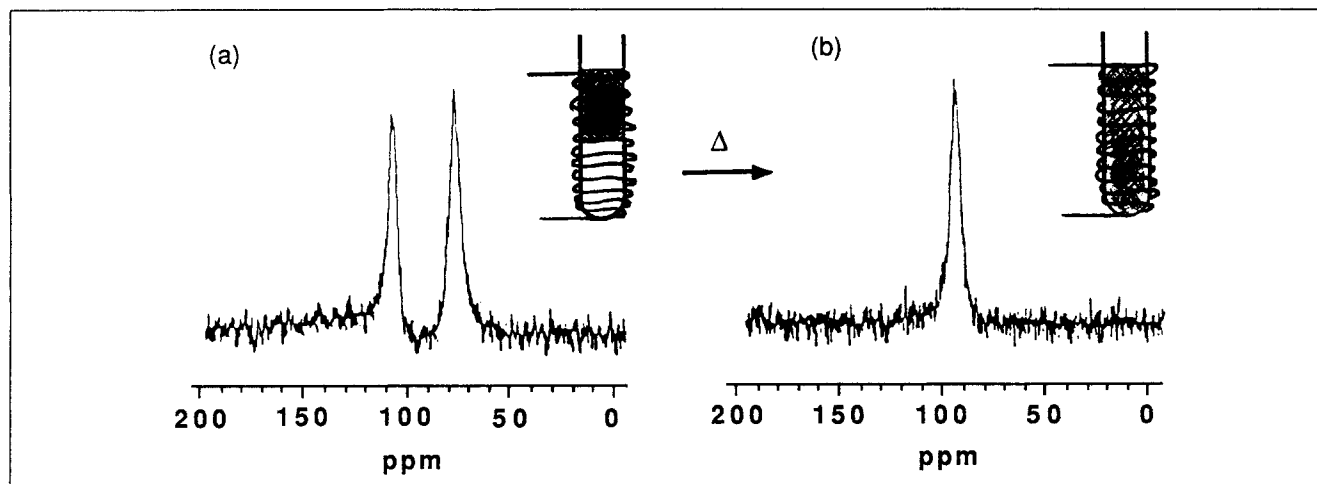


**Figure 1.** Room-temperature  $^{129}\text{Xe}$  NMR spectra of xenon [300 torr (40 kPa) equilibrium pressure] adsorbed on dehydrated NaY zeolite containing a bulk average of 0.5 HMB molecules per supercage.

(a) After heating the zeolite sample at 523 K for 2 h.

(b) After reheating the sample at 573 K for 4 h.

Schematic diagrams of NaY zeolite samples in 10 mm NMR tubes accompany the spectra. The receiver coil is shown to indicate the approximate sample volume probed by the NMR experiment. Shading reflects the concentration of adsorbed HMB guests in supercage environments.

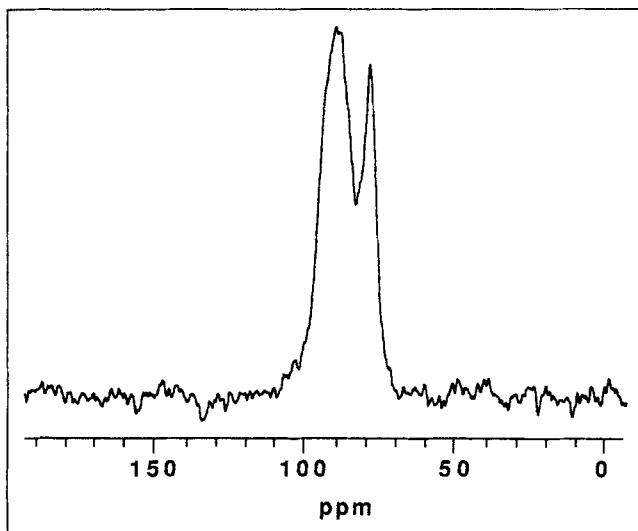


**Figure 2.** Room-temperature  $^{129}\text{Xe}$  NMR spectrum of xenon [300 torr (40 kPa) equilibrium pressure] adsorbed on partially hydrated NaY zeolite containing a bulk average of 0.5 HMB molecules per supercage.

The sample was dehydrated at 723 K for 5 h and then rehydrated uniformly to  $\approx 20\%$  of maximum NaY water content. HMB was added to the top of the bed and the system heated at 523 K for 2 h.

## Modeling Adsorbate Transport in NaY

### Sharp adsorption fronts

Modeling guest transport effects in porous solids is crucial to understanding guest/lattice interactions which influence the distribution of organic adsorbates in zeolites. Ruckenstein et al. (1971) and others (Garg and Ruthven, 1974; Doong and Yang, 1987) have modeled the sorption behavior of solids with bidisperse pore structures, formally similar to the packed bed of NaY crystallites considered here, and established the criteria necessary for identifying rate-limiting features of guest transport in these systems. The distribution of adsorbed guest species in a zeolite packed bed depends on the adsorption properties of the system, together with the relative transport rates of the guest species in the interstitial void spaces between the micron-sized crystallites (NaY macropores) and in the supercages and windows within individual zeolite crystallites (NaY micropores). Xenon-129 NMR provides a particularly useful means of probing adsorbed guest distributions in zeolites from which it is possible to estimate the relative time scales associated with adsorbed guest transport in bidispersed NaY pore systems.

At 523 K, the sharp HMB adsorption front observed in Figure 1a arises predominantly from diffusion of vapor-phase HMB molecules through the interstitial macropores separating the NaY crystallites, not through liquid-phase imbibition. Vapor-phase diffusion of HMB is confirmed experimentally by  $^{129}\text{Xe}$  NMR data from HMB/NaY samples prepared at 473 K in the absence of direct contact between the zeolite bed and liquid adsorbate (Chmelka, 1990).

To explain the sharp boundary between adsorption zones indicated in Figure 1a, we postulate that HMB molecules adsorb strongly from the vapor state onto the exterior surfaces of the NaY crystallites and migrate rapidly into interior cavities. In our nomenclature, strong adsorption refers to a high adsorp-

tion capacity by the zeolite support. Substantial mobility of adsorbed molecules through the nominal 0.8 nm windows from one supercage to another is permitted and, furthermore, is essential to explain the absence of pore-mouth blocking effects which would otherwise be severe for the large 0.82-nm-diameter HMB molecules. Moreover, we assert that at temperatures near 523 K, migration of strongly adsorbed organic guests within a 1- $\mu\text{m}$  crystallite occurs much faster than the rate at which the molecules diffuse in the gas phase through interparticle macropores to nascent crystallites.

Because NaY particles held at 523 K for 2 h sustain a kinetic barrier to adsorption of more than one HMB molecule per cavity (Chmelka, 1990), vapor-phase HMB molecules preferentially adsorb into unsaturated particles possessing a bulk loading of less than one HMB/supercage. After each supercage in a given 1- $\mu\text{m}$  particle has been loaded with a single HMB guest, subsequent vapor-phase HMB molecules diffuse past this saturated crystallite to the next unsaturated particle where they adsorb strongly and migrate rapidly into the crystallite's interior. Ultimately, the liquid HMB reservoir at the top of the bed is exhausted as all of the bulk organic material evaporates, diffuses, and chemisorbs as a mass-limited shock wave represented schematically in Figure 3a.

Three characteristic times exist for guest diffusion in a packed bed of microporous crystallites:  $t_{\text{micro}}$ , the time required for guest diffusion within a single crystallite;  $t_{\text{macro}}$ , the time required for guest diffusion in the bed macropores; and  $t_f$ , the time required for advance of the adsorption front through the bed. Formation of a sharp adsorption boundary between adsorption zones demands the following necessary and sufficient conditions:

$$t_f \gg t_{\text{macro}} \gg t_{\text{micro}} \quad (1)$$

Thus, a sharp adsorption front emerges only when both the diffusion rate in the NaY particles is fast compared to that in the interparticle macropores, and the macropore diffusion rate is fast compared to that for the advance of the adsorption zone. Transport of HMB in the intracrystalline micropores is fast compared to that in the macropores when  $t_{\text{macro}} \gg t_{\text{micro}}$  (Ruckenstein et al., 1971), or equivalently when

$$\frac{x_f^2}{D_{\text{macro}}} \gg \frac{d_p^2}{D_{\text{micro}}} \quad (2)$$

where  $d_p$  is the mean diameter of a NaY crystallite,  $x_f$  is the length of the adsorbate contact zone in the NaY packed bed,  $D_{\text{micro}}$  is the intracrystalline diffusivity of HMB within the micropores of a single crystallite, and  $D_{\text{macro}}$  is the intercrystalline diffusivity of HMB through the macropores between NaY crystallites. For the conditions of these experiments,  $d_p = 1 \mu\text{m}$ ,  $x_f = 1 \text{ cm}$ ,  $D_{\text{macro}} \approx 10^{-5} \text{ m}^2/\text{s}$  (Chmelka, 1990), allowing a lower bound on the intracrystalline diffusivity of the guest to be established. According to Ruckenstein et al. (1971), diffusion-limited transport in the macropores occurs when

$$\frac{x_f^2}{D_{\text{macro}}} > 100 \frac{d_p^2}{D_{\text{micro}}} \quad (3)$$

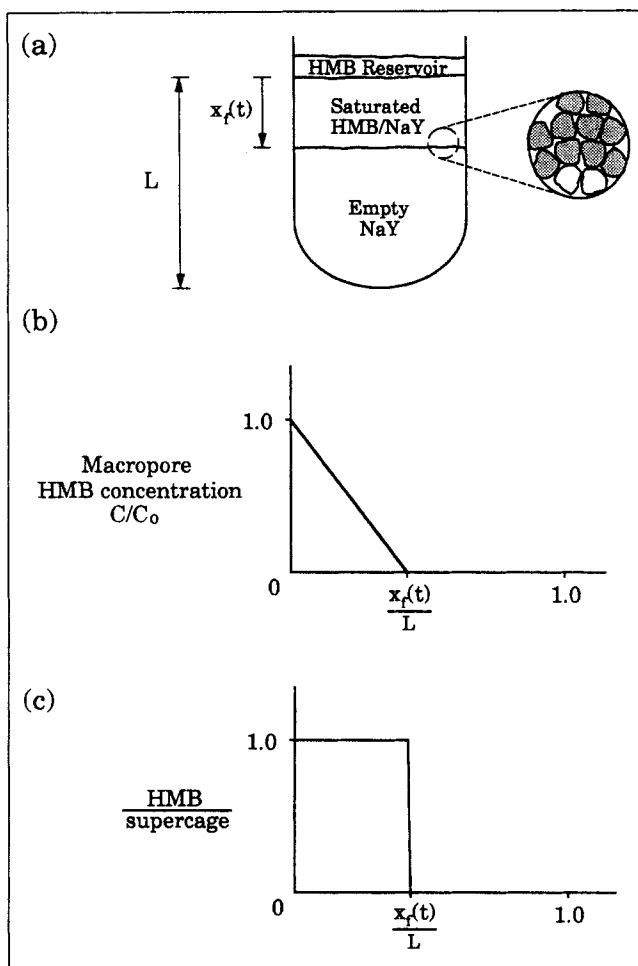


**Figure 3. (a) Axial HMB concentration profile at 523 K in the dehydrated NaY zeolite. The inset depicts the sharp boundary separating zones with and without adsorbed HMB. (b) Macropore HMB concentration vs. dimensionless distance from the top of the NaY bed. (c) Intracrystalline HMB loading in dehydrated NaY micropores vs. dimensionless distance from the top of the bed.**

yielding  $D_{\text{micro}} > 10^{-11} \text{ m}^2/\text{s}$  for HMB in dehydrated NaY at 523 K. This result is comparable to diffusivity data recently published for benzene in NaY (Förste et al., 1989).

When  $t_f \gg t_{\text{macro}}$ , diffusion in the packed-bed macropores follows a pseudosteady-state analysis (Froment and Bischoff, 1979). Consequently, a linear vapor-phase HMB concentration profile exists within the intercrystalline macropores of the HMB-saturated zone (Figure 3b), while the HMB concentration in the micropores of individual, dehydrated NaY crystallites is essentially uniform. This picture leads to an axial shrinking-core model (Froment and Bischoff, 1979), where the zone of no-adsorption is taken as the core. A material balance on the diffusing guest then leads to

$$\frac{\phi D_{\text{macro}} C_o}{x_f} = \alpha \frac{dx_f}{dt} \quad (4)$$

where  $x_f$  is the distance traveled by the guest adsorption front along the bed axis,  $\phi$  is the void fraction of the bed's macropores,  $C_o$  is the vapor-phase concentration of HMB in equilibrium with the liquid reservoir at the top of the bed, and  $\alpha$  is the adsorption capacity of the intracrystalline cavities expressed as moles of adsorbate per total bed volume. We take  $\alpha$  as a constant, consistent with the highly nonlinear adsorption isotherms for similar compounds such as benzene, *n*-heptane, and 1,3,5-triethylbenzene on faujasite-type zeolites (Dubinin et al., 1971; Dubinin et al., 1974; Breck, 1982).

Equation 4 is integrated to predict the time-dependent advance of the adsorption front through the zeolite bed:

$$t_f = \frac{x_f^2 \alpha}{2 \phi C_o D_{\text{macro}}} \quad (5)$$

Hence, the pseudosteady-state criterion,  $t_f \gg t_{\text{macro}}$  in Eq. 1, is satisfied when

$$\frac{\alpha}{\phi C_o} \gg 1, \quad (6)$$

or more specifically when (Bischoff, 1963; Bischoff, 1965; Luss, 1968; Theofanous and Lim, 1971; Froment and Bischoff, 1979)

$$\frac{\alpha}{\phi C_o} > 10^3. \quad (7)$$

For dehydrated NaY zeolite containing a bulk loading of 0.5 HMB/supercage chemisorbed at 523 K, the mass-limited adsorption front in NaY penetrates axially to the midpoint of the bed (Figure 3c), thus accounting for the two well-resolved  $^{129}\text{Xe}$  peaks in Figure 1a. For  $x_f = 1 \text{ cm}$  of contacted bed length,  $\alpha = 0.44 \text{ kmol HMB/m}^3 \text{ bed}$  (Chmelka, 1990),  $\phi \approx 0.5 \text{ m}^3 \text{ NaY/m}^3 \text{ bed}$ ,  $C_o = 2.3 \times 10^{-3} \text{ kmol/m}^3$  (Chmelka, 1990), and  $D_{\text{macro}} = 1.9 \times 10^{-5} \text{ m}^2/\text{s}$  (Chmelka, 1990), we calculate  $\alpha/(\phi C_o) \approx 770$  and  $t_f = 15 \text{ min}$ . These results are supported by separate experimental measurements on HMB/NaY samples held 5–10 minutes at 523 K, which indicate axial transport times of approximately 10 min (Chmelka, 1990).

The mass-limited nature of the HMB adsorption front at 523 K is confirmed in Figures 4a–c. The fraction of the zeolite bed saturated with one HMB guest molecule per supercage, determined from the integrated peak areas of the  $^{129}\text{Xe}$  spectra in Figures 4a–c, agrees with the overall bulk guest loadings of the respective samples. As the overall guest loading is increased from 0.25 to 0.50 and 0.93 HMB molecules per supercage, the larger adsorbate reservoirs supply the additional mass of HMB necessary for the deeper axial penetration of the front into the bed.

These observations hold true as well for adsorption of 1,3,5-trimethylbenzene in NaY at 323 K, which also establishes a sharp adsorption front for a loading of 0.5 TMB/supercage, as shown in Figure 5. While the axial HMB gradients correspond to systems far from thermodynamic equilibrium, such guest distributions are kinetically stable at room temperature over a period of many months (Chmelka, 1990). In general, the existence of a sharp adsorption boundary in a packed zeolite bed is anticipated when adsorption capacities are high for guest

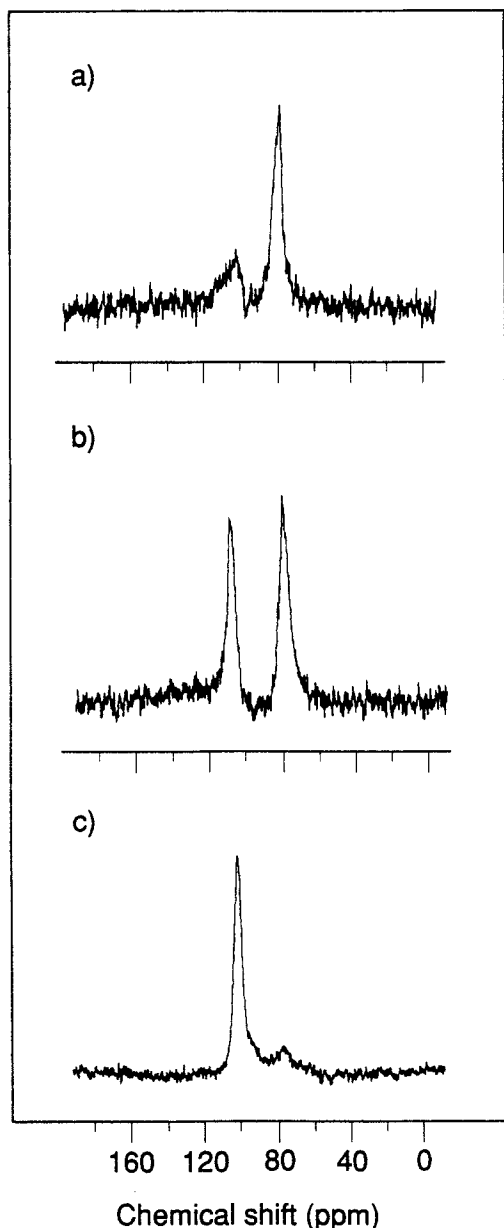


**Figure 4.** Room-temperature  $^{129}\text{Xe}$  NMR spectra of xenon [300 torr (40 kPa) equilibrium pressure] adsorbed on dehydrated NaY zeolite containing a bulk average of (a) 0.25, (b) 0.50, and (c) 0.93 HMB molecules per supercage.

Each sample was heated at 523 K for 2 h.

species possessing low vapor pressures and high intracrystalline mobilities in very small particles.

#### Effect of coadsorbed guests

The rate of intracrystalline HMB transport in the NaY micropores is dramatically reduced in the presence of even a small amount of previously adsorbed species such as water (see Figure 2). By creating a more crowded supercage environment, sorbed water obstructs migration of HMB guests within the NaY micropores. In this situation, the additional transport

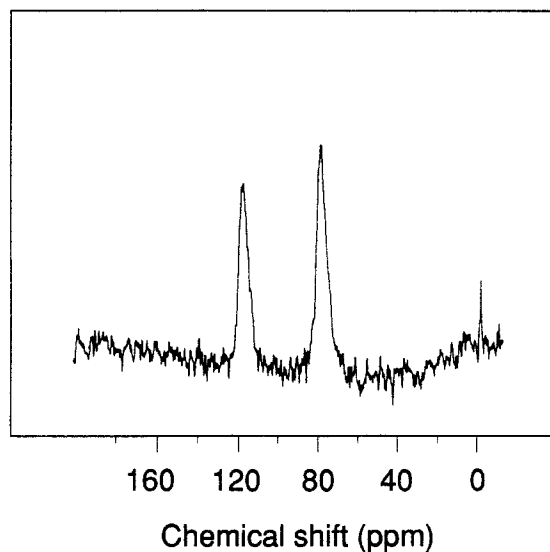


**Figure 5.** Room-temperature  $^{129}\text{Xe}$  NMR spectra of xenon [300 torr (40 kPa) equilibrium pressure] adsorbed on dehydrated NaY zeolite containing a bulk average of 0.50 TMB molecules per supercage after heating at 323 K for 0.5 h.

The peak observed at  $\approx 1$  ppm corresponds to gaseous  $^{129}\text{Xe}$ .

resistance can invalidate the condition of rapid intracrystalline transport, so that adsorbed HMB molecules migrate more slowly from the exterior crystallite surface to empty supercages in the particle interior. Intracrystalline transport of HMB in the micropores may, thus, proceed at a rate which is comparable to intercrystalline vapor-phase diffusion of HMB to the exterior surfaces of the NaY particles. Consequently,  $t_{\text{macro}} \approx t_{\text{micro}}$  or

$$\frac{x_f^2}{D_{\text{macro}}} \approx \frac{d_p^2}{D_{\text{micro}}}, \quad (8)$$

so that a shrinking-core model is no longer valid.  $D_{\text{micro}}$  is now estimated to be no larger than  $10^{-13} \text{ m}^2/\text{s}$  for HMB in 25% rehydrated NaY [5  $\text{H}_2\text{O}$ /supercage (Gedeon et al., 1988)]. Thus, the diffusivity of HMB in NaY decreases by at least two orders of magnitude in the presence of coadsorbed water. This is consistent with diffusivity data of Kärger and Pfeifer (1987) for low molecular weight hydrocarbons in partially hydrated NaY zeolite.

As in the case of the dehydrated HMB/NaY system discussed above, vapor-phase HMB molecules diffuse through the bed macropores until the HMB species adsorb on an unsaturated crystallite surface. The reduced intracrystalline mobility of HMB in partially hydrated NaY, however, results in substantially slower HMB migration into the zeolite particle interiors. Although a saturated surface region likely exists on the periphery of the NaY crystallites, the center cores are devoid of adsorbed HMB guests. Vapor-phase HMB molecules in the macropores perceive a saturated surface region in many partially hydrated crystallites that lack fully saturated interiors. The vapor-phase species diffuse through the macropores between NaY particles until contact is finally made with an unsaturated NaY crystallite surface. Under such conditions,

crystallites near the boundary between fully saturated and fully unsaturated regions of the bed possess a distribution of HMB loadings, as depicted schematically in Figure 6.

Intracrystalline adsorbate distributions in particles near the boundary likely evidence intraparticle shrinking-core behavior (Sohn and Szekely, 1972; Sohn and Szekely, 1974; Froment and Bischoff, 1979). The room-temperature  $^{129}\text{Xe}$  NMR technique, however, averages adsorbate distribution information within approximately one NaY crystallite (Chmelka, 1990), so that intracrystalline adsorbate concentration profiles are not accessible in this study. Nonetheless, the  $^{129}\text{Xe}$  NMR data of Figure 2 confirm that no sharp macroscopic adsorption front exists within the NaY packed bed. A transient macroscopic distribution of particles containing different HMB loadings is consistent with hindered intracrystalline transport of the HMB guests due to the presence of coadsorbed water. The axial shrinking-core

model no longer describes the chemisorption process in NaY powders when guest transport in the macropores and micropores occur at comparable rates (i.e., when  $t_{\text{macro}} \approx t_{\text{micro}}$ ).

### Guest dispersal at elevated temperatures

Chemisorption at higher temperatures increases the macropore concentration of the adsorbing species both by increasing the vapor pressure of the supply bulk liquid and by increasing the desorption rate of guest molecules. Under these circumstances, a more homogeneous macroscopic distribution of adsorbed guests is produced within the zeolite bed. At 573 K, for example,  $\alpha/(\phi C_0) \approx 140$  (Chmelka, 1990). Again, the axial shrinking-core model is inappropriate, since the relative adsorption capacity  $\alpha/(\phi C_0)$  is no longer sufficiently large to justify a pseudosteady-state treatment (i.e., now  $t_f \approx t_{\text{macro}}$ ) (Froment and Bischoff, 1979). The single  $^{129}\text{Xe}$  peak in Figure 1b reflects an average  $^{129}\text{Xe}$  environment resulting from rapid xenon exchange, in a single zeolite crystallite, between supercages with and without adsorbed HMB guest species (Chmelka, 1990). Thus, at 573 K HMB molecules are dispersed throughout the sample volume, and a sharp boundary between distinct macroscopic adsorption zones no longer exists. High guest concentrations in the macropores account for the dispersal of preadsorbed HMB/NaY documented in Figure 1b and observed separately from preadsorbed TMB and benzene on NaY as well (Chmelka, 1990; Chmelka et al., in press). These data are consistent with adsorption isotherms for 1,3,5-triethylbenzene on NaY that demonstrate substantially lower guest uptake at elevated temperatures where kinetic effects are unimportant (Dubinin et al., 1971; Dubinin et al., 1974; Breck, 1982).

### Conclusions

Transport of aromatic molecules, such as hexamethylbenzene, into a packed bed of micron-sized NaY crystallites at 523 K occurs predominantly by vapor-phase diffusion to exterior particle surfaces. HMB species adsorb strongly on NaY at temperatures near 523 K, migrating to interior supercages until all cavities contain approximately one molecular guest. The existence of a sharp adsorption front is predicated on an adsorption capacity that is large compared to the vapor-phase concentration of the diffusing organic material, coupled with rapid intracrystalline transport of adsorbed guest molecules. These two criteria specify an axial shrinking-core description of HMB diffusion in dehydrated NaY zeolite powder. The relative magnitudes of intracrystalline and vapor-phase intercrystalline guest transport rates, together with relative guest concentrations in the micropores and in the macropores, establish whether shrinking-core behavior will be observed.

In the absence of coadsorbed guests that hinder intracrystalline HMB transport, rapid migration of strongly adsorbed HMB within NaY micropores, relative to vapor-phase diffusion of HMB through the bed's macropores, produces a sharply defined adsorption front in a dehydrated NaY zeolite bed at 523 K. However, in the presence of a coadsorbed species such as water or at temperatures where the macropore guest concentration becomes important relative to the adsorbate concentration, no sharp adsorption front exists.

Xenon-129 NMR is a sensitive means of monitoring the macroscopic distributions of adsorbed guests in NaY zeolite produced by chemisorption at different temperatures. The

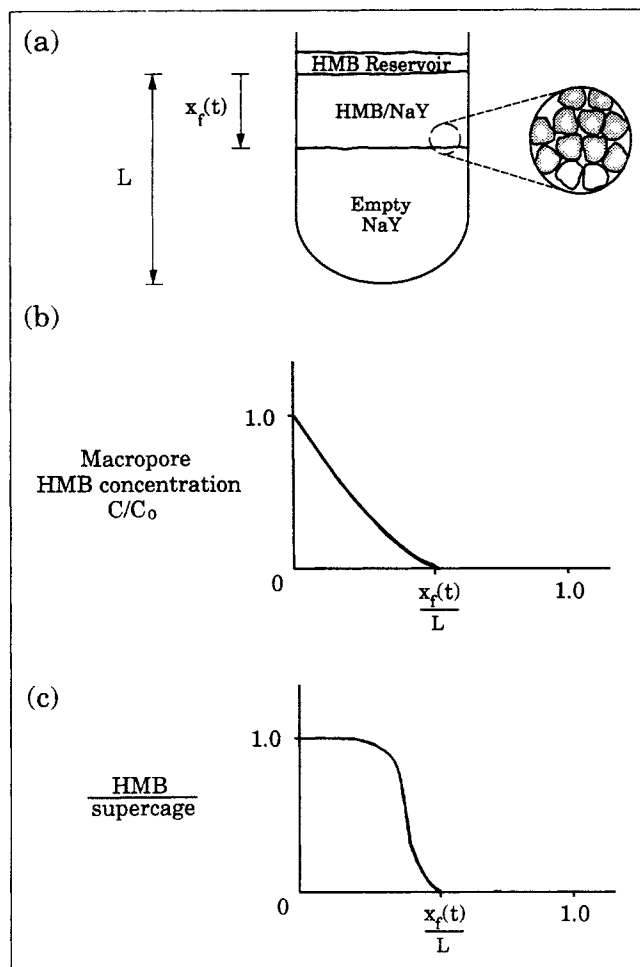


**Figure 6.** (a) Axial HMB concentration profile at 523 K in the rehydrated NaY zeolite. The inset depicts the indistinct boundary separating zones with and without adsorbed HMB. (b) Macropore HMB concentration vs. dimensionless distance from the top of the NaY bed. (c) Intracrystalline HMB loading in rehydrated NaY micropores vs. dimensionless distance from the top of the bed.

adsorbate distribution information obtained from  $^{129}\text{Xe}$  NMR complements the theoretical insight provided by the shrinking-core transport model. The result is a more quantitative description of molecular adsorption and transport processes in zeolites.

## Acknowledgment

The authors thank A. Pines for experimental support and L.C. de Menorval, S.B. Liu, and R. Ryoo for helpful discussions and experimental assistance.

## Notation

- $C$  = vapor-phase adsorbate concentration,  $\text{kmol}/\text{m}^3$   
 $C_o$  = vapor-phase adsorbate concentration in equilibrium with the liquid reservoir,  $\text{kmol}/\text{m}^3$   
 $d_p$  = NaY crystallite diameter, m  
 $D_{\text{macro}}$  = guest diffusivity in bed macropores separating zeolite crystallites,  $\text{m}^2/\text{s}$   
 $D_{\text{micro}}$  = guest diffusivity in NaY micropores within zeolite crystallites,  $\text{m}^2/\text{s}$   
 $L$  = length of packed bed, m  
 $t$  = time, s  
 $t_f$  = characteristic time for axial advances of the guest adsorption front through the bed, s  
 $t_{\text{macro}}$  = characteristic time for diffusion of guest molecules through the macropores, s  
 $t_{\text{micro}}$  = characteristic time for diffusion of guest molecules through the NaY micropores, s  
 $x_f$  = position of adsorption front measured from the top of the bed, m  
 $\alpha$  = intracrystalline zeolite adsorption capacity,  $\text{kmol}/\text{m}^3$   
 $\phi$  = void fraction of the macropores, dimensionless

## Literature Cited

- Bischoff, K. B., "Accuracy of the Pseudosteady-State Approximation for Moving Boundary Diffusion Problems," *Chem. Eng. Sci.*, **18**, 711 (1963).  
 ———, "Further Comments on the Pseudosteady-State Approximation for Moving Boundary Diffusion Problems," *Chem. Eng. Sci.*, **20**, 783 (1965).  
 Breck, D. W., *Zeolite Molecular Sieves*, Krieger, Malabar, FL (1982).  
 Chmelka, B. F., PhD Diss., University of California, Berkeley (1990).  
 Chmelka, B. F., J. G. Pearson, S. B. Liu, R. Ryoo, L. C. de Menorval, and A. Pines, "NMR Study of the Distribution of Aromatic Molecules in NaY Zeolite," *J. Phys. Chem.*, **95** in press (Jan., 1991).  
 Cohen de Lara, E., "Temperature Dependence of the Mobility of Adsorbed Molecules-Infrared Study," *Proc. Int. Conf. on Zeolites*, L. V. C. Rees, ed., Heyden, London, 414 (1980).  
 de Menorval, L. C., D. Raftery, S. B. Liu, K. Takegoshi, R. Ryoo, and A. Pines, "Investigations of Adsorbed Organic Molecules in NaY Zeolite by Xenon-129 NMR," *J. Phys. Chem.*, **94**, 27 (1990).  
 Doong, S. J., and R. T. Yang, "Bidisperse Pore Diffusion Model for Zeolite Pressure Swing Adsorption," *AIChE J.*, **33**, 1045 (1987).  
 Dubinin, M. M., K. M. Nikolaev, N. S. Polyakov, and N. I. Seregina, "Investigation of Adsorption of Vapors of Substances with Relatively

- Big Molecules: 2. Study of Activated Character of Adsorption on Active Charcoals," *Akad. Nauk SSSR, Izv., Ser. Khim.*, **1971**, 1871 (1971).  
 Dubinin, M. M., K. M. Nikolaev, N. S. Polyakov, N. I. Seregina, and Yu. A. Tokarev, "Study of Vapour Adsorption of Various Organic Substances: 3. Characteristics of the Microporous Structure of Adsorbents in Case of Activated Nature of Adsorption," *Akad. Nauk SSSR, Izv., Ser. Khim.*, **1974**, 1479 (1974).  
 Förste, C., J. Kärger, and H. Pfeifer, "Self-Diffusion by NMR Tracer Uptake Measurements," *Zeolites: Facts, Figures, Future, Stud. Surf. Sci. Catal.*, **49**, P. A. Jacobs and R. A. van Santen, eds., Elsevier, Amsterdam, 907 (1989).  
 Fraissard, J., T. Ito, L. C. de Menorval, and M. A. Spinguel-Huet, "Nuclear Magnetic Resonance Study of Xenon Adsorbed on Metal-NaY Zeolites (Size of Metal Particles and Chemisorption)," *Metal Microstructures in Zeolites: Preparation, Properties, Applications, Stud. Surf. Sci. Catal.*, **12**, P. A. Jacobs et al., eds. Elsevier, Amsterdam, 179 (1982).  
 Froment, G.F., and K. B. Bischoff, *Chemical Reactor Analysis and Reactor Design*, Wiley, New York, 242 (1979).  
 Garg, D. R., and D. M. Ruthven, "The Performance of Molecular Sieve Adsorption Columns: Systems with Micropore Diffusion Control," *Chem. Eng. Sci.*, **29**, 571 (1974).  
 Gedeon, A., T. Ito, and J. Fraissard, "Study of the  $\text{H}_2\text{O}/\text{NaY}$  System: an Example of the Application of  $^{129}\text{Xe}$  NMR of the Xenon Probe to the Investigation of the Location of Adsorbed Phases," *Zeolites*, **8**, 376 (1988).  
 Kärger, J., and H. Pfeifer, "N.M.R. Self-Diffusion Studies in Zeolite Science and Technology," *Zeolites*, **7**, 90 (1987).  
 Kärger, J., H. Pfeifer, M. Rauscher, M. Bülow, N. N. Samulevič, and S. P. Žandov, "Comparative NMR and Uptake Studies of Molecular Transport of Ethane in 5A Zeolites after Different Sample Treatments," *Zeit. Physik. Chem., Leipzig*, **262**, 567 (1981).  
 Kondis, E. F., and J. S. Dranoff, "Kinetics of Isothermal Sorption of Ethane on 4A Molecular Sieve Pellets," *Ind. Eng. Chem., Proc. Des. Develop.*, **10**, 108 (1971).  
 Luss, D., "On the Pseudosteady-State Approximation for Gas Solid Reactions," *Can. J. Chem. Eng.*, **46**, 154 (1968).  
 Ruckenstein, E., A. S. Vaidyanathan, and G. R. Youngquist, "Sorption by Solids with Bidisperse Pore Structures," *Chem. Eng. Sci.*, **26**, 1305 (1971).  
 Ryoo, R., S. B. Liu, L. C. de Menorval, K. Takegoshi, B. Chmelka, M. Trecocke, and A. Pines, "Distribution of Hexamethylbenzene in a Zeolite by Xenon-129 and Multiple-Quantum NMR," *J. Phys. Chem.*, **91**, 6575 (1987).  
 Sohn, H. Y., and J. Szekely, "The Effect of Intragrain Diffusion on the Reaction between a Porous Solid and a Gas," *Chem. Eng. Sci.*, **29**, 630 (1974).  
 ———, "Structural Model for Gas-Solid Reactions with a Moving Boundary: III. General Dimensionless Representation of the Irreversible Reaction between a Porous Solid and a Reactant Gas," *Chem. Eng. Sci.*, **27**, 763 (1972).  
 Theofanous, T. G., and H. C. Lim, "An Approximate Analytical Solution for Non-Planar Moving Boundary Problems," *Chem. Eng. Sci.*, **26**, 1297 (1971).

Manuscript received May 2, 1990, and revision received Aug. 20, 1990.